

Differentiating fluvial components of upper Canada Basin waters based on measurements of dissolved barium combined with other physical and chemical tracers

Christopher K. H. Guay¹, Fiona A. McLaughlin², and Michiyo Yamamoto-Kawai²

¹Pacific Marine Sciences and Technology, Oakland, California, USA

²Department of Fisheries and Oceans, Institute of Ocean Sciences, Sidney, British Columbia, Canada

Abstract

The utility of dissolved barium (Ba) as a quasi-conservative tracer of Arctic water masses has been demonstrated previously. Here we report distributions of salinity, temperature, and Ba in the upper 200 m of the Canada Basin and adjacent areas observed during cruises conducted in 2003-2004 as part of the Joint Western Arctic Climate Study (JWACS) and Beaufort Gyre Exploration Project (BGEF). A salinity-oxygen isotope mass balance is used to calculate the relative contributions from sea ice melt, meteoric, and saline end-members, and Ba measurements are incorporated to resolve the meteoric fraction into separate contributions from North American and Eurasian sources of runoff.

Large fractions of Eurasian runoff (as high as 15.5%) were observed in the surface layer throughout the Canada Basin, but significant amounts of North American runoff in the surface layer were only observed at the southernmost station occupied in the Canada Basin in 2004, nearest to the mouth of the Mackenzie River. Smaller contributions from both Eurasian and North American runoff were evident in the summer and winter Pacific-derived water masses that comprise the underlying upper halocline layer in the Canada Basin. Significant amounts of Eurasian and North American runoff were observed throughout the water column at a station occupied in Amundsen Gulf in 2004. This suggests the export of runoff from both sources through the passages of the Canadian Arctic Archipelago.

Keywords: Barium, Arctic rivers, Beaufort Gyre, Canada Basin, tracers

Index terms: 4800 Oceanography: Biological and chemical (0460); 4207 Arctic and Antarctic oceanography (9310, 9315); 4808 Chemical tracers; 4283 Water masses; 0744 Rivers (0483, 1856)

1. Introduction

The Canada Basin covers an area of approximately $1.6 \times 10^6 \text{ km}^2$ to the north of the Chukchi and Beaufort seas, accounting for $\sim 11\%$ of the total area of the Arctic Ocean. Low salinity surface waters of the Canada Basin comprise the largest reservoir of fresh water in the Arctic Ocean, with an inventory of approximately $25,600 \text{ km}^3$ of fresh water calculated for the upper 300 m of the water column in the Canada Basin relative to a reference salinity of 34.87 [Yamamoto-Kawai *et al.*, 2008]. The large fresh water content of the Canada Basin exerts a strong influence on the sea ice cover in the region – through its effect on salinity and water column stratification in areas of ice formation and its contribution to maintaining the cold halocline layer of the Arctic Ocean, which insulates sea ice from the heat contained in relatively warm, underlying waters of Atlantic origin [Shimada *et al.*, 2005; Björk *et al.*, 2002]. Fresh water contained in Canada Basin waters is exported via Fram Strait and the passages of the Canadian Arctic Archipelago (hereafter referred to simply as the Archipelago) to the Nordic Seas and Labrador Sea, where its contribution of positive buoyancy is one of the factors governing the extent of convective deep water formation in the North Atlantic [Aagaard and Carmack, 1989]. The fresh water cycle in the Canada Basin is therefore a significant component of the linkages between the Arctic system and global ocean circulation and climate.

Sources of fresh water to the Canada Basin include the influx of relatively fresh Pacific marine waters via Bering Strait, sea ice melt, river runoff, and net precipitation-minus-evaporation. These multiple sources of fresh water require other tracers in addition to salinity in order to differentiate them and determine their relative contributions to Canada Basin waters. A mass balance based on salinity and oxygen isotopes has been applied previously to determine proportions of meteoric water (*i.e.*, river runoff and precipitation), sea ice melt, and a marine

end-member in surface waters of the Canada Basin (Macdonald et al., 2002). Incorporating nutrient measurements (phosphate and nitrate/total inorganic nitrogen) differentiates marine waters of Atlantic and Pacific origin and allows separate Atlantic and Pacific marine end-members to be explicitly accounted for in the mass balance. [Jones et al., 1998; Yamamoto-Kawai et al., 2008]. Measurements of total alkalinity have been used to estimate the relative proportions of runoff contributed by the Eurasian arctic rivers and the Mackenzie River [Yamamoto-Kawai et al., 2005].

The utility of dissolved barium (Ba) as a quasi-conservative tracer of Canada Basin water masses has been demonstrated previously [Guay and Falkner, 1997; Guay et al., 1999]. Of particular interest is its application to differentiating runoff from Eurasian and North American sources based on the significant enrichment of Ba in North American arctic rivers relative to Eurasian arctic rivers [Guay and Falkner, 1997; Taylor et al., 2003; Cooper et al., 2008]. Here we present distributions of temperature, salinity and dissolved Ba in upper (depth ≤ 200 m) Canada Basin waters in summer 2003 and 2004. The salinity and Ba data are combined in a mass balance with oxygen isotope data from concurrent measurements [Yamamoto-Kawai et al., 2008] to determine the relative contributions of sea ice melt, Pacific water, and runoff from Eurasian and North American rivers.

2. Sample Collection and Analysis

Hydrographic stations were occupied in the Canada Basin and adjacent areas during research cruises on the *CCGS Louis S. St-Laurent* in summer 2003 and 2004 (Fig. 1). Water samples were collected from Niskin bottles deployed on a rosette equipped with a Sea-Bird Electronics SBE 9 CTD profiler. Bottle samples were analyzed for salinity using a Guildline Autosol salinometer referenced to IAPSO standard seawater.

Samples for Ba analysis were collected into trace metal clean HDPE bottles and prevented from freezing during transit and storage. Barium concentrations in the samples were determined on a VG Elemental ExCell quadrupole inductively coupled plasma mass spectrometer (ICP-MS) at the W. M. Keck Collaboratory for Plasma Spectrometry, College of Oceanic and Atmospheric Sciences, Oregon State University. An isotope dilution method was used that is similar to one described previously in more detail [Guay, 1997]. Briefly, 250- μ l aliquots of sample were spiked with an equal volume of a ^{135}Ba -enriched solution (Oak Ridge National Laboratories) and diluted with 10 ml of 1% HNO_3 . The ICP-MS was operated in peak jump mode, and data were accumulated over three 20-s intervals for masses 135 and 138. Based on replicate analyses of samples and standardized reference materials, the precision (2-sigma) of the analytical procedure ranges from $< 5\%$ at $10 \text{ nmol Ba l}^{-1}$ to $< 3\%$ at $100 \text{ nmol Ba l}^{-1}$.

3. Results

Distributions of salinity, temperature, and dissolved barium

In 2003 (Fig. 2), relatively fresh ($S < 31$), cold ($T < -1^\circ\text{C}$) waters were observed throughout the upper 50 m at the stations in the central Canada Basin. Surface salinity generally decreased moving from west to east across the basin, with lowest values (27-28) observed in the southeast (stations 36-38) and highest values observed in the northernmost region of the sampling area (stations 20-23). Dissolved Ba concentrations ranged between 60 and 79 nmol Ba l^{-1} , with higher values generally observed in the western region of the Canada Basin (particularly high concentrations were observed at stations 7, 24 and 25).

The stations over the shelf break north of Alaska (stations 2-4) were remarkable for the presence of a water mass characterized by highly elevated temperatures (up to 4.2°C) and extremely low Ba concentrations (as low as $32 \text{ nmol Ba l}^{-1}$) at depths between 10 m and 90 m.

The core of this feature was centered at approximately 50 m and extended to stations immediately northwards from the shelf break along transect A (stations 5-6) – but it was not observed at stations over the Chukchi shelf break to the west at the southern ends of transects E and F. Over the central Canada Basin, waters of intermediate salinity ($S = 29-32.5$) with moderately warm temperatures ($T > -1^{\circ}\text{C}$) and low Ba concentrations ($< 65 \text{ nmol Ba l}^{-1}$) were observed uniformly at depths between approximately 30 m and 80 m.

Beneath this layer, waters with salinity between 32.5 and 34, near-freezing temperatures, and elevated Ba concentrations ($65-75 \text{ nmol Ba l}^{-1}$) were observed at depths between 75 m and 175 m throughout the sampling area and appeared to shoal continuously to the surface at the stations near the Chukchi shelf break in the vicinity of the Chukchi Borderland (southern/western ends of transects D, E and F). At lower depths (150-200 m) along all of the transects, the appearance of higher salinity waters ($S > 34$) was observed in association with temperatures elevated with respect to immediately overlying waters ($T > -1^{\circ}\text{C}$) and low Ba concentrations ($40-55 \text{ nmol Ba l}^{-1}$). These waters were most prevalent at stations in the northern region of the sampling area and also appeared to shoal slightly at stations over the shelf break and the southern portion of the Chukchi Borderland (*e.g.*, stations 2, 13, and 14).

A similar pattern of salinity, temperature and dissolved barium distributions was observed in 2004 (Fig. 3). Surface waters over the central Canada Basin were characterized by low salinity (< 31 , with values of 26-27 or lower commonly observed throughout the sampling area), cold temperatures ($T < -1^{\circ}\text{C}$), and Ba concentrations of $60-70 \text{ nmol Ba l}^{-1}$ in the upper 50 m of the water column. In general, upper Canada Basin waters were fresher in 2004 relative to 2003. This may be partly due to differences in the geographical distributions of sampling locations in the two years, but the overall trend is consistent with direct comparisons between individual

stations occupied in the exact same locations during the 2003 and 2004 cruises – *e.g.*, station 8 in 2003 and station 4 in 2004; station 33 in 2003 and station 18 in 2004; etc. In addition, low-salinity surface waters were observed at two stations in the southeast Canada Basin closer to the shelf break than any of the stations occupied in the area in 2003. At station 28, extremely fresh ($S = 24.3-24.5$), warm ($T > 5^{\circ}\text{C}$) waters highly elevated in Ba ($119 \text{ nmol Ba l}^{-1}$) were observed in the upper 15 m of the water column. At station 1, the upper 15 m of the water column was also characterized by relatively low salinity values ($26.7-27.9$), but temperature (-1.0 to 0.8°C) and Ba ($66 \text{ nmol Ba l}^{-1}$) were only slightly elevated compared to waters over a similar depth range at nearby stations.

A layer of warm ($T > -1^{\circ}\text{C}$) water with intermediate salinity ($29.0-32.5$) was again observed throughout most of the Canada Basin at depths between 30 m and 80 m. While transect A in 2004 did not extend as far south over the shelf break and slope as it did in 2003, waters with highly elevated temperatures ($> 1^{\circ}\text{C}$) with a core centered at ~ 50 m were observed at the southernmost end of the transect (stations 2-7). The concentrations of Ba associated with these waters appeared to be higher ($> 65 \text{ nmol Ba l}^{-1}$) relative to 2003. Another notable difference from the 2003 distributions is the observation at some stations (*e.g.*, stations 14-15 and 19-23) of a separate, thinner layer of warm water above the warm water mass with its core at ~ 50 m.

Consistent with observations in 2003, waters with salinity between 32.5 and 34, near-freezing temperatures, and relatively high Ba concentrations ($65-75 \text{ nmol Ba l}^{-1}$) were observed at depths of 75 to 175 m throughout the Canada Basin. Below this water mass, higher salinity waters ($S > 34$) with temperatures elevated relative to immediately overlying waters ($T > -1^{\circ}\text{C}$) and low Ba concentrations ($40-55 \text{ nmol Ba l}^{-1}$) were present at depths of 150-200 m. As observed in 2003, these waters were most prevalent at these depths at stations in the northern

region of the sampling area. Waters with these characteristics were also evident at the stations nearest the shelf break in the southeast Canada Basin (stations 1, 28 and 30).

In 2004, a station was also occupied in Amundsen Gulf (70° 33' N, 122° 54' W, water depth ~650 m; labeled “AG” on Fig. 1), which lies to the southeast of the Canada Basin and constitutes a major entrance to the passages of the Archipelago. Surface waters (0-20 m) at this station were characterized by extremely low salinity (20-30) and warm temperatures (1.0-1.4°C), and the Ba concentration of the single water sample collected in this depth range was 65 nmol Ba l⁻¹ (Fig. 4). As depth decreased between 20 m and 125 m, salinity increased from 30.0 to 33.1. Temperature decreased from 0.6°C to a minimum value of -1.5°C at 97 m, rising back to -1.4°C at 125 m. Elevated Ba concentrations were observed at these depths, decreasing from a value of 86 nmol Ba l⁻¹ at 25 m to a value of 75 nmol Ba l⁻¹ at 125 m. Between depths of 125 m and 200 m, salinity increased from 33.1 to 34.4 and temperature increased from -1.4 °C to -0.2 °C. Dissolved Ba concentrations in the samples from this depth range decreased from 70 nmol Ba l⁻¹ at a depth of 145 m to 56 nmol Ba l⁻¹ at a depth of 205 m.

Composition of upper Canada Basin waters based on salinity-oxygen isotope mass balance

Salinity and oxygen isotope measurements (reported in *Yamamoto-Kawai et al.*, 2008) were used to calculate the composition of the samples collected from the upper 200 m at the hydrographic stations occupied in 2003 and 2004 (Figs. 5-7). Adopting the convention used by others in previous work (*e.g.*, *Östlund and Hut*, 1984; *Bauch et al.*, 1995; *Macdonald et al.*, 2002; *Yamamoto-Kawai et al.*, 2008), upper Canada Basin waters were assumed to contain a mixture of three end-members: sea ice melt, meteoric (comprising precipitation as well as runoff from Eurasian and North American rivers), and saline (a mixture of Pacific and Atlantic source waters). The values of salinity and $\delta^{18}\text{O}$ assigned to sea ice melt, meteoric water, Atlantic water

and Pacific water are those used by *Yamamoto-Kawai et al.*, 2008 (Table 1). For samples with salinity ≤ 33 (*i.e.*, collected from above the nutrient maximum in the Canada Basin; *Jones et al.*, 1991) the saline end-member was assumed to contain only Pacific water and is therefore assigned the salinity and $\delta^{18}\text{O}$ values of Pacific water. For samples with salinity > 33 , the saline end-member is assumed to contain a mixture of Pacific and Atlantic waters in a ratio calculated from nutrient measurements (reported in *Yamamoto-Kawai et al.*, 2008) according to the method described in *Jones et al.*, 1998:

$$P_{\text{Atl}} = (N_{\text{obs}} + 3.072) / 17.499, \quad (1)$$

$$P_{\text{Pac}} = (N_{\text{obs}} + 11.306) / 13.957, \quad (2)$$

$$R_{\text{mix}} = (P_{\text{obs}} + P_{\text{Atl}}) / (P_{\text{Pac}} + P_{\text{Atl}}), \quad (3)$$

where N_{obs} and P_{obs} are the nitrate and phosphate concentrations measured in the water sample, P_{Atl} is the phosphate concentration calculated using the nitrate:phosphate relationship for Atlantic water reported in *Jones et al.*, 1998, P_{Pac} is the phosphate concentration calculated using the modified nitrate:phosphate relationship for Pacific water reported in *Yamamoto-Kawai et al.*, 2008, and R_{mix} is the ratio of Pacific water to Atlantic water in the saline end-member (the uncertainty in the calculated values of R_{mix} is estimated to be < 0.14). The salinity and $\delta^{18}\text{O}$ values for the mixed saline end-member are then calculated according to the following equations:

$$S_s = S_{\text{PW}} * R_{\text{mix}} + S_{\text{AW}} * (1 - R_{\text{mix}}) \quad (4)$$

$$\delta_s = \delta_{\text{PW}} * R_{\text{mix}} + \delta_{\text{AW}} * (1 - R_{\text{mix}}) \quad (5)$$

The proportion of the sea ice melt, meteoric, and saline end-members contained in each sample is determined by solving the following mass balance equations for salt and $\delta^{18}\text{O}$:

$$f_i + f_m + f_s = 1, \quad (6)$$

$$f_i S_i + f_m S_m + f_s S_s = S_{\text{obs}}, \quad (7)$$

$$f_i \delta_i + f_m \delta_m + f_s \delta_s = \delta_{\text{obs}}, \quad (8)$$

where f , S , and d represent the fraction, salinity and $\delta^{18}\text{O}$ values of the end-members (the subscripts i , m , and s correspond to sea ice melt, meteoric, and saline end-members, respectively) and S_{obs} and δ_{obs} are the salinity and $\delta^{18}\text{O}$ values measured for each water sample. The uncertainties in the calculated values of f_i , f_m , and f_s (due to the precision of the $\delta^{18}\text{O}$ measurements (± 0.04 ‰ or lower), the uncertainties in the end-member S and $\delta^{18}\text{O}$ values, and the uncertainty in the values calculated for R_{mix}) are estimated to be 0.03, 0.03 and 0.14, respectively.

Determination of Eurasian and North American runoff contributions based on dissolved barium measurements

Runoff to the Arctic Ocean from North American rivers is significantly elevated in dissolved Ba relative to runoff from Eurasian rivers (Table 2). This reflects the differences in the distributions of rock types in the watersheds of these rivers (Guay, 1997). It is therefore possible to incorporate dissolved Ba measurements with results from the salinity-oxygen isotope mass balance to resolve the meteoric fraction into contributions from Eurasian and North American river runoff (Figs. 8-10). In using this approach, it is necessary to assume that the meteoric fraction of upper Canada Basin waters is composed entirely of river runoff (*i.e.*, no significant contribution from net precipitation) and that Ba behaves conservatively. While these assumptions may lead to inaccuracies for waters that have been altered significantly by intense seasonal biological activity and/or received large amounts of direct precipitation (*e.g.*, coastal waters and ice-free surface waters in the Chukchi Sea during summer), it should provide reasonable results for waters in which biological drawdown is minimal and Ba behaves

conservatively (*e.g.*, areas beneath the ice cover in the interior Canada Basin). The fractions of Eurasian and North American runoff are calculated from the following mass balance equations:

$$f_E + f_N = f_m, \quad (9)$$

$$f_i[\text{Ba}]_i + f_s[\text{Ba}]_s + f_E[\text{Ba}]_E + f_N[\text{Ba}]_N = [\text{Ba}]_{\text{obs}}, \quad (10)$$

where f_E and f_N are the fractions of Eurasian and North American runoff, f_i , f_s , and f_m are the fractions of the sea ice melt, saline, and meteoric end-members calculated previously from the salinity-oxygen isotope mass balance (Equations 1-8), $[\text{Ba}]_i$, $[\text{Ba}]_s$, $[\text{Ba}]_E$ and $[\text{Ba}]_N$ are the dissolved Ba concentrations of the sea ice melt, saline, Eurasian runoff and North American runoff end-members, and $[\text{Ba}]_{\text{obs}}$ is the dissolved Ba concentration measured for each water sample.

A value of $5 \pm 1 \text{ nmol Ba l}^{-1}$ is used for the dissolved Ba concentration of the sea ice melt end-member (*Guay and Falkner, 1997; Taylor et al., 2003*). For samples with salinity ≤ 33 , the saline end-member is assumed to contain only Pacific water and is therefore assigned the dissolved Ba concentration of Pacific water ($55 \pm 5 \text{ nmol Ba l}^{-1}$; *Guay and Falkner, 1997*). For samples with salinity > 33 , the saline end-member is assumed to contain a mixture of Pacific and Atlantic waters. The dissolved Ba concentration for the mixed saline end-member is then calculated according to the following equation:

$$[\text{Ba}]_s = [\text{Ba}]_{\text{PW}} * R_{\text{mix}} + [\text{Ba}]_{\text{AW}} * (1 - R_{\text{mix}}) \quad (11)$$

where $[\text{Ba}]_s$ is the dissolved Ba concentration of the mixed saline end-member, $[\text{Ba}]_{\text{PW}}$ is the dissolved Ba concentration of Pacific water, $[\text{Ba}]_{\text{AW}}$ is the dissolved Ba concentration of Atlantic water ($43 \pm 3 \text{ nmol Ba l}^{-1}$; *Guay and Falkner, 1997*), and R_{mix} is the mixing ratio of Pacific water to Atlantic water in the sample determined previously from nutrient measurements.

Choosing values of dissolved Ba concentration for the river runoff end-members is complicated by the enhancement of dissolved Ba in estuaries due to desorption of Ba^{2+} from suspended fluvial particles upon encountering seawater cations at increasing salinities [Edmond *et al.*, 1978; Carroll *et al.*, 1993]. An effective river end-member dissolved Ba concentration can be determined by constructing a plot of [Ba] vs. salinity for samples collected throughout the estuary and extrapolating the linear portion of the Ba-salinity trend back to its intercept on the [Ba] axis at salinity = 0. This provides a more accurate assessment of the actual amount of dissolved Ba delivered to ocean waters by river discharge and typically results in an effective river end-member [Ba] value significantly higher than the dissolved Ba concentrations measured in river water samples collected above the estuary (Table 2).

The Mackenzie River is the largest river entering the Arctic Ocean from North America. The effective river end-member [Ba] value determined for the Mackenzie River based on samples collected through the salinity gradient in the estuary is $520 \text{ nmol Ba l}^{-1}$ [Guay and Falkner, 1998]. This is significantly higher than the flow-weighted average dissolved Ba concentration of $371 \text{ nmol Ba l}^{-1}$ observed in Mackenzie River waters collected above the estuary over a multi-year sampling period [Cooper *et al.*, 2008]. Similar dissolved Ba concentrations were measured in river water samples collected above the salinity gradient in the Yukon River ($371 \text{ nmol Ba l}^{-1}$; Cooper *et al.*, 2008) and the Colville River ($369 \text{ nmol Ba l}^{-1}$; Rember and Trefry, 2004), which is the largest river draining into the Arctic from the north slope of Alaska. Although no data are available from the estuaries of these rivers, it is assumed that the enhancement of dissolved Ba due to the desorption of Ba^{2+} ions from suspended particles is similar to that observed for the Mackenzie River. A value of $520 \text{ nmol Ba l}^{-1}$ is therefore chosen as the effective dissolved Ba concentration for the North American runoff end-member.

Flow-weighted average dissolved Ba concentrations are significantly lower in the four largest rivers entering the Arctic Ocean from Eurasia: the Lena (104 nmol Ba l⁻¹), Ob (141 nmol Ba l⁻¹), Yenisey (76 nmol Ba l⁻¹), and Kolyma (63 nmol Ba l⁻¹) [Cooper *et al.*, 2008]. The flow-weighted average values for the Lena and Ob rivers are significantly higher than dissolved Ba concentrations reported previously for these rivers based on a more limited set of samples [Guay and Falkner, 1998]. It is therefore likely that the effective river end-member [Ba] values determined by Guay and Falkner (1998) for the Lena and Ob rivers (130 nmol Ba l⁻¹ and 100 nmol Ba l⁻¹, respectively) underestimate the actual dissolved Ba loads associated with runoff from these rivers. The effective river end-member [Ba] value determined by Guay and Falkner (1998) for the Yenisey River (125 nmol Ba l⁻¹) appears reasonable in light of the agreement between their reported range of dissolved Ba concentrations (20-110 nmol Ba l⁻¹) and the flow-weighted average dissolved Ba concentration (76 nmol Ba l⁻¹) reported by Cooper, *et al.*, 2008. Based on these data and the relative sizes of the mean annual discharges of these rivers (Table 2), a value of 130 nmol Ba l⁻¹ is chosen as the effective dissolved Ba concentration for the Eurasian runoff end-member.

To assess the sensitivity of the mass balance to the values of [Ba] chosen for the North American and Eurasian runoff end-members, the calculations were performed while varying the range of the reported values by $\pm 15\%$ (*i.e.*, 440-600 nmol Ba l⁻¹ for the North American runoff end-member and 110-150 nmol Ba l⁻¹ for the Eurasian runoff end-member). This resulted in changes of ≤ 0.02 to the calculated values of f_N and f_E . By comparison, varying the values of [Ba] for Pacific water, Atlantic water, and the sea ice melt end-member over their reported ranges of uncertainty resulted in changes of ≤ 0.02 , ≤ 0.008 , and ≤ 0.001 , respectively, to the calculated values of f_N and f_E .

4. Discussion

Surface mixed layer

Relatively fresh ($S < 31$), near-freezing ($T < -1^{\circ}\text{C}$) waters characteristic of the surface layer in the western Arctic Ocean (*e.g.*, the Polar Surface Layer defined in *Morison et al.*, 1996) were observed in the upper 50 m of the water column throughout the interior Canada Basin in 2003 and 2004. In general, upper Canada Basin waters were fresher in 2004 relative to 2003. This may be partly due to differences in the geographical distributions of sampling locations in the two years, but the overall trend is consistent with direct comparisons between individual stations occupied in the exact same locations during the 2003 and 2004 cruises – *e.g.*, station 8 in 2003 and station 4 in 2004; station 33 in 2003 and station 18 in 2004; etc. In addition, low-salinity surface waters were observed at two stations in the southeast Canada Basin closer to the shelf break than any of the stations occupied in the area in 2003. At station 28, extremely fresh ($S = 24.3\text{-}24.5$), warm ($T > 5^{\circ}\text{C}$) waters highly elevated in Ba ($119 \text{ nmol Ba l}^{-1}$) were observed in the upper 15 m of the water column. At station 1, the upper 15 m of the water column was also characterized by relatively low salinity values ($26.7\text{-}27.9$), but temperature (-1.0 to 0.8°C) and Ba ($66 \text{ nmol Ba l}^{-1}$) were only slightly elevated compared to waters over a similar depth range at nearby stations.

The surface layer in the central Canada Basin contained significant amounts of both meteoric water and sea ice melt, with the meteoric component generally much larger than the sea ice melt component (highest meteoric fractions were 1.5-2 times greater than the highest sea ice melt fractions). In both 2003 and 2004, the meteoric fraction was $> 9\%$ in the upper 50 m of the water column throughout the sampling area, decreasing steadily with depth in subsurface waters (Figs. 5- 6). Excluding an exceptionally high value (24%) observed for the uppermost sample (6

m) at the southern end of transect B (station 28) in 2004, the range of values observed for the meteoric fraction in the upper 50 m was slightly lower in 2004 (upper quartile: 12-15%) compared to 2003 (upper quartile: 13-15%). Highest values ($> 12\%$) were also confined to a less extensive area in the southern and eastern areas of the Canada Basin in 2004 relative to 2003.

In contrast, much higher sea ice melt fractions were widely observed in 2004 relative to 2003 (especially in the southern regions of the Canada Basin). In 2003, the sea ice melt fraction in the upper 20-30 m of the water column over the central Canada Basin generally ranged between 0% and 2%, with exceptionally high values (2-6%) observed in the southeast region of the sampling area in the vicinity of the Beaufort Sea (stations 37-38; Fig. 5). In 2004, sea ice melt fractions $> 4\%$ were observed throughout the sampling area at similar depths, reaching values as high as 9-10% at the southern ends of transect A (station 2) and transect B (station 29; Fig. 6). This suggests that the freshening observed in surface waters in the sampling area from 2003 to 2004 was primarily due to increased sea ice melt, which is consistent with observations of accelerating rates of reduction in sea ice extent and concentration in the Canada Basin since the late 1990s [Shimada *et al.*, 2006].

The meteoric fraction of surface waters in the sampling area was dominated by Eurasian runoff in both years. In 2003, the fraction of Eurasian runoff was greater than 12% in the upper 35 m over the southern and central regions of the Canada Basin, with highest values (14-15%) observed near the surface at stations 7, 33 and 37 (Fig. 8). In 2004, Eurasian runoff fractions greater than 12% were once again observed in the upper 35 m of the water column in the Canada Basin, but they were confined to a smaller area relative to 2003 (Fig. 9). With a few exceptions (*e.g.*, the uppermost sample at station 3 along transect A), Eurasian runoff fractions above 12% were only observed east of 145°W longitude and south of 75°N latitude. At stations occupied in

the western region of the Canada Basin (transect A and the western end of transect D), the Eurasian runoff fraction observed in the upper 35 m in 2004 was lower relative to measurements made in similar locations in 2003 (*e.g.*, the Eurasian runoff fraction was 9-12% in samples collected from depths above 25 m at station 3 in 2004, while values of 13-15% were observed in samples collected from depths above 25 m at station 7 in 2003). In both years, the Eurasian runoff fraction remained above 6% down to depths of 50 m throughout the sampling area.

In 2003, none of the stations in the Canada Basin contained significant amounts of North American runoff in the upper 50 m (the fraction of North American runoff ranged between -2% and 2%, which is indistinguishable from zero within the level of uncertainty of the mass balance calculations; Fig. 8). In 2004, the presence of North American runoff in the upper 50 m was evident only in the uppermost sample (depth = 5 m) collected at the southernmost station occupied in the Canada Basin (station 28; Fig. 9). The significant North American runoff fraction in this sample (12%), coupled with extremely low salinity (24.5), high temperature (5.5°C), and high [Ba] (119 nmol l⁻¹) associated with this sample, along with the geographical location of station 28, suggest the influence of discharge from the Mackenzie River. Waters with similar properties were not observed in any of the samples from greater depths (≥ 25 m) at station 28, nor were they observed any depths at neighboring stations along transects B and D. It therefore appears that surface waters containing discharge from the Mackenzie River were confined to the extreme south of the Canada Basin and adjacent areas over the shelf in 2003 and 2004. This is consistent with the findings of *Yamamoto-Kawai et al.*, 2005, which indicated that a significant source of meteoric water besides North American runoff is required to account for the distribution of alkalinity observed in the southern Canada Basin.

Summer Bering Strait inflow

Two distinct types of summertime Pacific source waters to the Canada Basin have been identified [Steele *et al.*, 2004; Shimada *et al.*, 2001; Coachman *et al.*, 1975], both of which enter the basin at depths below the fresher, less dense surface layer and contribute to the upper halocline: Alaskan Coastal Water (ACW), which flows through the eastern side of Bering Strait and continues northward in a narrow coastal current, and summer Bering Sea Water (sBSW), which is a combination of Bering Shelf Water and Gulf of Anadyr Water that occupies the central Chukchi Sea and is strongly influenced by seasonal heating and freshening.

During its transit through the eastern Bering and Chukchi seas, ACW is warmed due to high summertime insolation and freshened from large contributions of runoff, particularly from the Yukon River. ACW enters the Canada Basin primarily through Barrow Canyon, where a portion is diverted northwards into the interior of the basin [Weingartner *et al.*, 1998; Coachman *et al.*, 1975] while the rest is transported eastward in a subsurface boundary current towards the Beaufort Sea [Steele *et al.*, 2004; Aagaard, 1984]. The relatively cooler, more saline sBSW flows primarily northward from the Chukchi Sea into the Canada Basin via Herald Canyon and the Central Channel (also referred to as Hanna Trough), although some amount is entrained into the flow of ACW through Barrow Canyon. Steele *et al.*, 2004, report temperature and salinity ranges of 0-6°C and 31-32 for ACW and 0-2°C and 32-33 for sBSW. Lower salinities were observed for both types of water by Woodgate and Aagaard, 2005, in Bering Strait, with a range of 29.0-31.5 in the buoyant ACW in the upper 35 m near the Alaskan coast and a range of 31.5-32.5 in the rest of the waters occupying the eastern half of the strait between Alaska and the Diomedes Islands.

The layer of relatively warm waters observed between approximately 30 m and 80 m throughout the Canada Basin in 2003 and 2004 is associated with summertime Pacific inflow

through Bering Strait. In our results from 2003, ACW was evident as the mass of exceptionally warm ($2.0^{\circ}\text{C} < T < 4.2^{\circ}\text{C}$) water occupying depths of 10-90 m at stations 2-4 over the shelf break east of Barrow Canyon. The highly depleted Ba concentrations measured in these waters reflect the biological uptake of Ba from surface waters in the eastern Bering and Chukchi seas during the summertime period of intense productivity [Guay and Falkner, 1998; Falkner et al., 1994]. The ACW signal was attenuated but still obvious in the temperature and Ba distributions at station 6 located ~200 km beyond the shelf break along transect A, northeast of Barrow Canyon. The presence of two distinct subsurface temperature maxima at station 6 suggests a combination of ACW overlying sBSW [Steele et al., 2004] entrained in the inflow through Barrow Canyon and/or advected from entry points further to the west along the Chukchi shelf break. In 2004, warm waters characterized by two separate subsurface temperature maxima were again observed at depths of 15-90 m in offshore waters northeast of Barrow Canyon (although there was no obvious evidence of waters extremely depleted in Ba as was observed in 2003) and at stations in the southern and eastern region of the sampling area. Throughout the Canada Basin, the properties of the warm layer observed at depths of 30-80 m in both years was consistent with a mixture of ACW and sBSW, with the prevalence of ACW decreasing with distance away from the transport pathway of ACW through Barrow Canyon and the eastward boundary current over the slope north of Alaska.

Relatively high sea ice melt (> 2%) and significant amounts of meteoric water (up to 12%) extended from the surface to depths as great as 80 m over the shelf break at the southern end of transect A (stations 2-4), which is consistent with their formation over the Bering and Chukchi shelves during the summer. The influence of waters with these properties was evident in the warm layer present at depths of 30-80 m throughout the Canada Basin in 2003 and 2004. The

mass balance incorporating Ba measurements suggest that most of the meteoric fraction in these waters is attributable to Eurasian runoff, while contributions from North American runoff are small or negligible. This is consistent with a large contribution to this layer by sBSW, which is formed in regions of the Chukchi Sea influenced by the eastward transport of shelf waters from the adjacent East Siberian Sea. The fraction of North American runoff may be underestimated, however, as a result of the non-conservative depletion of Ba observed in the ACW inflow, which transports the bulk of the discharge from the Yukon River. The extreme negative values (-3% to -6 %) calculated for the fraction of North American runoff at stations west of Barrow Canyon in 2003 are a result of the low Ba concentrations measured in these waters that were attributed to biological drawdown associated with high summertime productivity in the eastern Bering and Chukchi seas. The period of maximum productivity coincides with the period of highest flows in the Yukon River, when the majority of its discharge is entrained in the northward flux of ACW through Bering Strait. If large amounts of Ba are stripped from a significant portion of the ACW inflow to the Canada Basin during this period, a mass balance based on a North American runoff end-member with $[Ba] = 520 \text{ nmol Ba l}^{-1}$ would not sufficiently capture the contribution from the Yukon River.

Winter Bering Strait inflow

Winter Bering Sea Water (wBSW) constitutes a third type of Pacific source water to the Canada Basin [Steele *et al.*, 2004; Coachman *et al.*, 1975]. This water mass resides below ACW and sBSW in the Canada Basin halocline and is characterized by near-freezing temperatures and a nutrient maximum centered at a salinity of 33.1 [Jones and Anderson, 1986]. The properties of wBSW are conditioned by ice formation and brine rejection occurring in its source regions over the Bering and Chukchi shelves during the winter. Remineralization of sediments deposited

during the period of high productivity in the summer may also contribute to the relatively high nutrient levels characteristic of this water mass.

In 2003 and 2004, wBSW was evident at depths of 100-200 m throughout sampling area as a layer of cold ($T < -1^{\circ}\text{C}$), Ba-enriched ($65\text{-}75 \text{ nmol Ba l}^{-1}$) waters with its core situated around the 33.1 isohaline. The fraction of sea ice melt within this layer was highly negative (-4% to -8%), indicating the influence of sea ice formation on wBSW. The prevalence of extremely low values ($< -6\%$) at stations in the vicinity of the Chukchi shelf break are consistent with a source region over the Bering and Chukchi shelves. Similarly low values were also observed at stations in the vicinity of the Beaufort shelf break, suggesting that waters formed over the Beaufort shelf in winter may have also contributed to this layer in the Canada Basin. The absence of waters with these properties at the stations occupied over the Chukchi Borderland in 2003 (transect F) provides further evidence that this layer comprises inputs from the Bering, Chukchi, and/or Beaufort seas, as opposed to waters advected eastward from areas of formation over the Eurasian shelves.

In both 2003 and 2004, the fraction of meteoric water in this layer was generally between 3% and 6% and decreased steadily with depth. The Eurasian runoff fraction ranged from 0% to 5% in both years, with comparable values (0-5%) observed for the fraction of North American runoff. With the exception of a limited number of surface samples, this is the only layer where positive North American runoff fractions (*i.e.*, clearly distinguishable from zero given the reported level of uncertainty) were regularly observed. While this is consistent with the geographical proximity of North American rivers to the areas where wBSW is formed, it is possible that the amount of North American runoff contained in this layer was overestimated by the mass balance. The processes of ice formation/brine rejection and sediment remineralization

responsible for the nutrient maximum observed in wBSW could also lead to enrichment of Ba in these waters, which would result in the calculation of artificially high North American runoff fractions.

Export via the Canadian Arctic Archipelago

The station occupied in the Amundsen Gulf in 2004 gives an indication of the composition of waters exported from the southern Canada Basin through the passages of the Archipelago. The upper 20 m of the water column were warm and very fresh, containing a large fraction of sea ice melt and significant amounts of runoff from Eurasian and North American sources (Figs. 7, 10). For the only sample collected from this depth range (5 m), the sea ice melt fraction was 25% and the meteoric fraction was 11%, with roughly 2.5 times as much Eurasian runoff as North American runoff (8% and 3%, respectively). These properties could have resulted from a mixture of surface waters from the interior Canada Basin (dominated by Eurasian runoff), surface waters from the Beaufort Sea influenced strongly by North American runoff (particularly from the Mackenzie River), and a large pulse of meltwater from sea ice melted locally during the summer season.

The temperature decreased rapidly at depths below 20 m, remaining near freezing down to ~125 m. The meteoric fraction dropped from 11% to 6% over this depth range, with the Eurasian runoff component steadily decreasing (7% to 2%) while the North American runoff fraction remained roughly constant (~4%). The prevalence of North American runoff contained in these waters indicates that they did not result simply from advection of cold surface waters from the interior Canada Basin, and the influence of net sea ice formation was evident from the highly negative values of sea ice melt fraction in all samples collected from this depth range (-7% to -9%). This suggests the presence of a winter water mass from a source region strongly

impacted by North American runoff – *i.e.*, formed locally or advected from the adjacent regions of the Beaufort Sea.

Temperature increased steadily at depths below 125 m. In the samples collected between 145 m and 205 m, the sea ice melt fraction was negative (-1% to -4%) but not as low as values in the immediately overlying waters. The meteoric fraction in these waters was relatively low ($\leq 2\%$), with negative values calculated by the mass balance for the Eurasian runoff fraction. Salinity at these depths (33.1-34.4) was well above the range of summertime Pacific waters (ACW and sBSW), indicating that mixing with underlying Atlantic waters was the source of the warming observed in this layer.

The areas encompassed by the profiles of Eurasian runoff fraction and North American runoff fraction in the upper 200 m at this station (Fig. 10) were similar, suggesting that roughly comparable amounts of Eurasian runoff and North American runoff were transported over all depths in the waters exported from the Canada Basin eastwards through the Amundsen Gulf. While this observation represents a one-time sampling at a single location and does not account for temporal variability in the magnitude and direction of flow through the Amundsen Gulf, it provides evidence in support of a significant transport pathway by which North American runoff exits the Arctic to the North Atlantic via the Archipelago. This is consistent with our overall results from 2003 and 2004, which indicated that North American runoff was largely confined to nearshore regions of the southern Canada Basin instead of being transported offshore and becoming incorporated in the Beaufort Gyre, where it would be available for export to the North Atlantic via Fram Strait.

Relationship between atmospheric forcing and transport of fluvial discharge

Due to the sensitive coupling between Arctic atmospheric and oceanic circulation, it is necessary to consider the variability in atmospheric forcing when assessing the degree to which the 2003-2004 observations in the Canada Basin are representative of long-term conditions. The basin-scale atmospheric forcing regime in the Arctic has been described by an Arctic Oscillation (AO) index based on the leading EOF of wintertime sea level pressure poleward of 20°N [Thompson and Wallace, 1998]. This pattern of sea level pressure variability can be interpreted as surface signature of modulations in the strength of the stratospheric polar vortex: Positive values of the AO index are associated with a strong polar vortex and low sea level pressure over the central Arctic, and vice versa.

Starting in 1989, the AO index shifted into a period of persistent, high positive values that lasted through 1995. A complex series of interrelated responses in ocean circulation were observed in conjunction with this shift in atmospheric forcing, including the greater penetration of warm Atlantic waters into the central Arctic Ocean [Carmack *et al.*, 1995; Carmack *et al.*, 1997; Morison *et al.*, 1998], movement of the axis of the Transpolar Drift from a position over the Lomonosov Ridge to a position over the Mendeleev Ridge [Carmack *et al.*, 1995; McLaughlin *et al.*, 1996; Morison *et al.*, 1998], the reduction of the area occupied by the Beaufort Gyre and the retreat of its core towards the southern Canada Basin, and the disappearance of the cold halocline layer from the Nansen, Amundsen and Makarov basins [Steele and Boyd, 1998]. The overall ocean response to atmospheric forcing embodied by positive and negative phases of the AO has been described by cyclonic and anticyclonic ocean circulation regimes, respectively, which are related to patterns of sea surface height in the Arctic Ocean [Proshutinsky and Johnson, 1997].

The value of the AO index became negative again in 1996 and has generally remained negative since then (although positive values were observed in 1997, 2000, 2002, and 2007). This has been accompanied by a shift to the anticyclonic mode of ocean circulation and the relaxation of conditions to pre-1990s conditions -- *e.g.*, the retreat of Atlantic waters towards the Eurasian Basin and the return of the Transpolar Drift axis to the Lomonosov Ridge [Morison *et al.*, 2006; Alkire *et al.*, 2007], strengthening of the Beaufort Gyre, and a partial recovery of the cold halocline in the Nansen, Amundsen and Makarov basins [Boyd *et al.*, 2002; Björk *et al.*, 2002].

The transport and fate of Eurasian river runoff also varies with atmospheric forcing conditions. In a positive AO/cyclonic oceanic circulation regime, the large amount of runoff discharged to the Laptev and East Siberian seas (from the Lena River in particular) tends to be confined to nearshore waters and flow eastward along the shelf. Storage of Eurasian runoff over the Laptev and East Siberian shelves increases [Dmitrenko *et al.*, 2008; Steele and Ermold, 2004] and the primary insertion point of Eurasian shelf waters into the central Arctic moves eastwards to the East Siberian Sea, accompanying the shift of the Transpolar Drift axis towards the Mendeleev Ridge [Guay *et al.*, 2001; Schlosser *et al.*, 2002; Newton *et al.*, 2008]. Steele and Boyd, 1998, explained the retreat of the cold halocline from the Eurasian basin observed in the early-to-mid 1990s as a result of the eastward diversion of Eurasian runoff associated with the predominantly positive AO conditions prevailing during the period. Conversely, these conditions would favor the transport of Eurasian runoff towards the Chukchi Sea and Canada Basin.

In a negative AO/anticyclonic ocean circulation regime, Eurasian runoff tends to be transported directly across-shelf from the river mouths towards the interior Arctic basins

[*Dmitrenko et al., 2008; Steele and Ermold, 2004*]. The delivery of Eurasian runoff to the central Arctic increases, and the primary insertion point of Eurasian shelf waters moves westwards towards the Laptev Sea, accompanying the movement of the Transpolar Drift axis towards the Lomonosov Ridge. The increased supply of Eurasian runoff to the Eurasian Basin associated with the persistence of anticyclonic ocean conditions since 1997 has been put forth as an explanation of the partial recovery of the cold halocline in the region observed from 1998-2001 [*Boyd et al., 2002; Björk et al., 2002*]. These conditions would not be favorable to the direct transport of Eurasian runoff eastwards towards the Chukchi Sea and Canada Basin.

While this idealized relationship between Eurasian runoff transport and basin-scale atmospheric forcing provides a useful first-order description, it does not fully capture the complexity of the real system. The East Siberian Sea is a dynamic zone of interaction between Eurasian shelf waters and Pacific waters from a branch of the Bering inflow that enters via westward flow from the Chukchi Sea [*Semiletov et al., 2005; Jones et al., 1998*]. High variability has been observed in both the speed and direction of currents flowing between the Chukchi, East Siberian and Laptev seas [*e.g., Weingartner et al., 1999; Munchow et al., 1999*], and the importance of local wind conditions (especially during the summertime period of maximum river discharge) in determining the transport pathways of Eurasian runoff has been demonstrated [*Guay et al., 2001; Dmitrenko et al., 2005*].

Regardless of the state of basin-scale atmospheric forcing (positive or negative AO index) or ocean circulation regime (cyclonic or anticyclonic), significant amounts of Eurasian runoff can be transported to the Canada Basin by entrainment of Transpolar Drift waters into the adjacent Beaufort Gyre and/or direct inflow of shelf waters from the East Siberian Sea and adjacent areas of the Chukchi Sea in the region between the southern terminus of the

Mendeleyev Ridge and the Chukchi Borderland. This also implies that, under any conditions, Eurasian runoff will be contained in waters exported from the Arctic through Fram Strait and the Archipelago. This is consistent with our observations of large fractions of Eurasian runoff in surface waters throughout the sampling area (including the Amundsen Gulf) in 2003-2004 in spite of the prevailing negative AO index and anticyclonic ocean circulation regime during this period.

With respect to North American source of runoff to the Canada Basin, the transport pathways of contributions from the Yukon and Mackenzie rivers must be considered separately. The majority of discharge from the Yukon River (and other rivers flowing into the eastern Bering and Chukchi seas from western Alaska) is entrained in the swift, shallow, narrow flow of ACW that hugs the western Alaskan coast and enters the Canada Basin via subsurface flow through Barrow Canyon and the eastward subsurface boundary current paralleling the shelf/slope north of Alaska. *Steele et al.*, 2004, observed that ACW was entrained in the compressed Beaufort Gyre and eastward boundary current in the southern Canada Basin during the period of strongly positive AO index in the late 1980s and early 1990s. They speculated that ACW (and therefore Yukon runoff) would be largely confined to the southern Canada Basin during periods of positive AO/cyclonic conditions, where its only available exit route to the North Atlantic would be via the Archipelago; whereas during periods of negative AO/anticyclonic conditions, ACW would be more broadly distributed throughout the Beaufort Gyre and could become incorporated in waters exiting the Arctic through Fram Strait as well as the Archipelago. Our observations in 2003 and 2004 (during negative AO conditions) show no indications of Yukon runoff in areas of the Beaufort Gyre away from the southern/eastern Canada Basin, but its presence may not have been obvious in the tracer distributions – especially if biological

drawdown of Ba from summertime surface waters in the eastern Bering and Chukchi seas resulted in the underestimation of Yukon contributions to the North American runoff fraction. Under either atmospheric/oceanic circulation regime, Yukon runoff is largely incorporated into the upper halocline layer and does not contribute significantly to the surface layer in the Canada Basin.

Runoff from the Mackenzie River (and, to a lesser extent, from rivers draining the north slope of Alaska) will tend to be steered eastwards after leaving the river mouth and accumulate over the Beaufort Shelf and adjacent areas of the southeastern Canada Basin, where its only available export pathway to the North Atlantic will be via the Archipelago. This mechanism is consistent with results from a transect across Fram Strait in 1998, during which significant amounts of Eurasian runoff but no detectable North American runoff were observed in waters exiting the Arctic in the upper East Greenland Current [*Taylor et al.*, 2003].

During periods when local winds favorable to offshore transport persist over the Beaufort Sea in summer/fall (*i.e.*, when the runoff content of shelf waters is highest), Mackenzie runoff can be transported offshore into the Canada Basin. This was observed during the Surface Heat Budget of the Arctic Ocean (SHEBA) experiment in 1997, when a low-salinity anomaly formed in the southern Beaufort Gyre [*Macdonald et al.*, 1999; *McPhee et al.*, 1998]. Measurements of salinity, oxygen isotopes, and dissolved Ba demonstrated that the source of the excess freshwater was primarily runoff from the Mackenzie River [*Macdonald et al.*, 1999; *Macdonald et al.*, 2002]. Subsequent modeling studies confirmed that wind-driven northwestward advection of water from the Mackenzie Delta in 1997-2000 created the freshwater anomaly, which persisted until 2002 [*Steele et al.*, 2006]. The model results also indicated that over roughly the past three

decades (1978-2004), wind-driven northwest transport offshore from the Mackenzie Delta in summer/fall was an anomalous condition (observed in 1978-82, 1990, 1995, and 1997-2000).

The transport of Mackenzie runoff to the Beaufort Gyre associated with the formation and maintenance of the freshwater anomaly occurred after the shift from positive AO to negative AO that occurred in 1996. The Mackenzie runoff would have therefore been entrained into a strong, expanded Beaufort Gyre, with the possibility of exiting the Arctic via Fram Strait as well as being exported through the Archipelago (note that since the low-salinity anomaly first appeared in the southern Beaufort Gyre in 1997, any associated Mackenzie runoff signal would not have had sufficient time to reach Fram Strait by the time that the transect described by *Taylor et al.*, 2003, was occupied in late summer/fall of 1998).

It must be remembered, however, that the occurrence of negative AO/anticyclonic ocean circulation conditions do not necessarily imply that Mackenzie runoff will be entrained in Beaufort Gyre waters and subsequently exported through Fram Strait. If the anomalous winds driving offshore transport from the Beaufort Sea are not also present, Mackenzie runoff will remain in nearshore waters over the shelf and flow eastward into the Archipelago. This situation is characterized by our 2003 and 2004 observations, which showed no signs of Mackenzie runoff beyond nearshore waters in the vicinity of the Beaufort Sea and Amundsen Gulf in spite of the anticyclonic ocean circulation regime prevalent at the time.

Alternatively, during periods when cyclonic ocean conditions prevail, Mackenzie runoff can still be transported to the Beaufort Gyre if local winds favorable to offshore transport persist over the Beaufort Sea. But the Beaufort Gyre will be compressed and pushed back towards the southern Canada Basin, making its waters (along with any entrained Mackenzie runoff) more

likely to be exported through the Archipelago instead of exiting the Arctic with Transpolar Drift waters via Fram Strait.

5. Conclusions

These results further demonstrate the utility of dissolved Ba, in combination with other physical and geochemical tracers, for investigating Arctic Ocean circulation. Of particular value is the ability of dissolved Ba to differentiate runoff from North American and Eurasian sources. Our observations indicate that Eurasian runoff dominated the fraction of meteoric water contained in the surface layer in the Canada Basin in 2003 and 2004. Runoff from the Yukon River was incorporated into Alaskan Coastal Water, a summer Pacific water mass that flows in a shallow, buoyant current in the eastern Bering and Chukchi seas and enters the Canada Basin below the surface layer via flow through Barrow Canyon and an eastward boundary current that parallels the slope north of Alaska. The non-conservative drawdown of Ba from surface waters in the eastern Bering and Chukchi seas associated with intense summertime productivity in these areas makes it difficult to explicitly account for Yukon runoff in the fraction of North American runoff determined by incorporating dissolved Ba measurements with results from a salinity-oxygen isotope mass balance. Based on the signature of Alaskan Coastal Water in the 2003-2004 salinity and temperature distributions, it was inferred that the majority of Yukon runoff becomes entrained in upper halocline waters and does not contribute significantly to the surface layer in the Canada Basin. Runoff from the Mackenzie River was confined to the Beaufort Sea and adjacent areas of the southeastern Canada Basin in 2003 and 2004, flowing eastward through the Canadian Arctic Archipelago to ultimately be exported to the North Atlantic in the vicinity of the Labrador Sea. This is presumed to be the prevalent pathway for Mackenzie runoff, but the transport of waters northwestward from the Mackenzie Delta to the Beaufort Gyre can occur

when anomalous wind conditions drive offshore transport from the Beaufort Sea. It is evident that the pathways by which runoff from different sources enters the circulation of the Canada Basin and ultimately becomes exported to the North Atlantic depends strongly on both regional wind conditions in summer/fall and the prevalent basin-scale atmospheric forcing and ocean circulation regimes. Ongoing analyses of additional samples collected in 2005-2008 will establish a multi-year time series and provide further insight into the transport and fate of fluvial discharge within the Canada Basin.

Acknowledgments

Thanks to Sarah Zimmermann (Fisheries and Oceans Canada, Institute of Ocean Sciences) and the crew of the *CCGS Louis S. St-Laurent* for collecting the water samples and CTD data described in this study. Andy Ungerer and Robert Collier (College of Oceanic and Atmospheric Sciences, Oregon State University) provided facilities and assistance with the ICP-MS analyses. Comments from two anonymous reviewers led to significant improvements in the manuscript. Support for this research was provided by the National Science Foundation, Office of Polar Programs (OPP-0230184).

References

- Aagaard, K., and E.C. Carmack (1989), The role of sea ice and other fresh water in the Arctic circulation, *J. Geophys. Res.*, *94*, 14,485–14,498.
- Aagaard, K. (1984), The Beaufort Undercurrent, in *The Alaskan Beaufort Sea*, edited by P.W. Barnes et al., pp. 47–71, Academic Press, Inc., Orlando, Fla.
- Alkire, M.B., K.K. Falkner, I. Rigor, M. Steele, and J. Morison (2007), The return of Pacific waters to the upper layers of the central Arctic Ocean, *Deep Sea Res. Part I*, *54*, 1509–1529.
- Bauch, D., P. Schlosser, and R. Fairbanks (1995), Freshwater balance and sources of deep and bottom water in the Arctic Ocean inferred from the distribution of H₂¹⁸O, *Progr. Oceanogr.*, *35*, 53–80.
- G. Björk, J. Söderkvist, P. Winsor, A. Nikolopoulos, and M. Steele, Return of the cold halocline layer to the Amundsen Basin of the Arctic Ocean: Implications for the sea ice mass balance, *Geophys. Res. Lett.*, *29*(11), 1513, 10.1029/2001GL014157.
- Boyd, T.J., M. Steele, R.D. Muench, and J.T. Gunn (2002), Partial recovery of the Arctic Ocean halocline, *Geophys. Res. Lett.*, *29*(14), 1657, 10.1029/2001GL014047.
- Carmack, E.C., R.W. Macdonald, R.G. Perkin, F.A. McLaughlin, and R.J. Pearson (1995), Evidence for warming of Atlantic water in the southern Canadian Basin of the Arctic Ocean: Results from the Larsen-93 expedition, *Geophys. Res. Lett.*, *22*, 1061–1064.
- Carmack, E.C., K. Aagaard, J.H. Swift, R.W. Macdonald, F.A. McLaughlin, E.P. Jones, R.G. Perkin, J.N. Smith, K.M. Ellis, and L. Kilius (1997), Changes in temperature and tracer distributions within the Arctic Ocean: results from the 1994 Arctic Ocean section, *Deep Sea Res. Part II*, *44*, 1487–1502.
- Carroll, J., K.K. Falkner, E.T. Brown, and W.S. Moore (1993), The role of sediments in maintaining high dissolved ²²⁶Ra and a in the Ganges-Brahmaputra mixing zone, *Geochim. Cosmochim. Acta*, *57*, 2981–2990.
- Coachman, L.K., K. Aagaard, and R.B. Tripp (1975), Bering Strait: The Regional Physical Oceanography, Univ. of Wash. Press, Seattle.
- Cooper, L.W., R. Benner, J.W. McClelland, B.J. Peterson, R.M. Holmes, P.A. Raymond, D.A. Hansell, J.M. Grebmeier, and L.A. Codispoti (2005), Linkages among runoff, dissolved organic carbon, and the stable oxygen isotope composition of seawater and other water mass indicators in the Arctic Ocean, *J. Geophys. Res.*, *110*, G02013, doi:10.1029/2005JG000031.
- Cooper, L.W., J.W. McClelland, R.M. Holmes, P.A. Raymond, J.J. Gibson, C.K. Guay, and B.J. Peterson (2008), Flow-weighted Tracer Content ($\delta^{18}\text{O}$, DOC, Ba, Alkalinity) of the Six Largest Arctic Rivers, *Geophys. Res. Lett.*, in press.

Dmitrenko, I.A., S.A. Kirillov, and L.B. Tremblay, The long-term and interannual variability of summer fresh water storage over the eastern Siberian shelf: Implication for climatic change, *J. Geophys. Res.*, *113*, C03007, doi:10.1029/2007JC004304.

Dmitrenko, I., S. Kirillov, H. Eicken, and N. Markova (2005), Wind-driven summer surface hydrography of the eastern Siberian shelf, *Geophys. Res. Lett.*, *32*, L14613, doi:10.1029/2005GL023022

Edmond, J.M, E.D. Boyle, D. Drummond, B. Grant, and T. Mislick (1978), Desorption of barium in the plume of the Zaire (Congo) River, *Neth. J. Sea Res.*, *12*, 324–328.

Eicken, H., H.R. Krouse, D. Kadko, and D.K. Perovich (2002), Tracer studies of pathways and rates of meltwater transport through Arctic summer sea ice, *J. Geophys. Res.*, *107*(C10), 8046, doi:10.1029/2000JC000583.

Ekwurzel, B., P. Schlosser, R. Mortlock, R. Fairbanks, and J. Swift (2001), River runoff, sea ice meltwater, and Pacific water distribution and mean residence times in the Arctic Ocean, *J. Geophys. Res.*, *106*, 9075–9092.

Falkner, K.K., R.W. Macdonald, E.C. Carmack, and T. Weingartner (1994), The potential of barium as a tracer of Arctic water masses, in *The Polar Oceans and Their Role in Shaping the Global Environment*, *Geophys. Monogr. Ser.*, vol. 85, edited by O.M. Johannessen et al., pp. 63–76, AGU, Washington, D.C.

Guay, C.K., G.P. Klinkhammer, K.K. Falkner, R. Benner, P.G. Coble, T.E. Whitledge, B. Black, F.J. Bussel, and T.A. Wagner (1999), High-resolution measurements of dissolved organic carbon in the Arctic Ocean by *in situ* fiber-optic spectrometry, *Geophys. Res. Lett.*, *26*(8), 1007–1010.

Guay, C.K.H. (1997), Barium as a tracer of Arctic halocline and river waters, M.S. thesis, Oregon State Univ., Corvallis, 1997.

Guay, C.K., and K.K. Falkner (1997), Barium as a tracer of Arctic halocline and river waters, *Deep Sea Res. Part II*, *44*, 1543–1569.

Guay, C.K., and K.K. Falkner (1998), A survey of dissolved barium in the estuaries of major Arctic rivers and adjacent seas, *Cont. Shelf Res.*, *18*(8), 859–882.

Guay, C.K.H., K.K. Falkner, R.D. Muench, M. Mensch, M. Frank, and R. Bayer (2001), Wind-driven transport pathways for Eurasian Arctic river discharge, *J. Geophys. Res.*, *106*(C6), 11,469–11,480.

Jones, E.P., L.G. Anderson, and J.H. Swift (1998), Distribution of Atlantic and Pacific waters in the upper Arctic Ocean: Implications for circulation, *Geophys. Res., Lett.*, *25*, 765–768.

Jones, E.P. and L.G. Anderson (1986), On the origin of the chemical properties of the

Arctic Ocean halocline. *J. Geophys. Res.*, *91*, 10759–10767.

Jones, E.P., Anderson, L.G., and Wallace, D.W.R. (1991), Tracers of near-surface, halocline and deep waters in the Arctic Ocean: Implications for circulation. *J. Mar. Syst.*, *2*, 241–255.

Macdonald, R.W., F.A. McLaughlin, and E.C. Carmack (2002), Fresh water and its sources during the SHEBA drift in the Canada Basin of the Arctic Ocean, *Deep Sea Res. Part I*, *49*, 1769–1785.

Macdonald, R.W., E.C. Carmack, F.A. McLaughlin, K.K. Falkner, and J.H. Swift, (1999), Connections among ice, runoff, and atmospheric forcing in the Beaufort Gyre, *Geophys. Res. Lett.*, *26*(15), 2223–2226.

McLaughlin, F.A., E.C. Carmack, R.W. Macdonald, and J.K.B. Bishop (1996), Physical and geochemical properties across the Atlantic/Pacific water mass front in the southern Canada Basin, *J. Geophys. Res.*, *101*, 1183–1197.

McPhee, M.G., T.P. Stanton, J.H. Morison, and D.G. Martinson (1998), Freshening of the upper ocean in the Arctic: Is perennial sea ice disappearing?, *Geophys. Res. Lett.*, *25*, 1729–1732.

Morison, J., M. Steele, and R. Andersen (1998), Hydrography of the upper Arctic Ocean measured from the nuclear submarine *USS Pargo*, *Deep Sea Res. Part I*, *45*, 15–38.

Morison, J., M. Steele, T. Kikuchi, K. Falkner, and W. Smethie (2006), Relaxation of central Arctic Ocean hydrography to pre-1990s climatology, *Geophys. Res. Lett.*, *33*, L17604, doi:10.1029/2006GL026826.

Munchow, A., T.J. Weingartner, and L.W. Cooper (1999), The summer hydrography and surface circulation of the East Siberian shelf sea, *J. Phys. Oceanogr.*, *29*, 2167–2182.

Newton, R., P. Schlosser, D. G. Martinson, and W. Maslowski (2008), Freshwater distribution in the Arctic Ocean: Simulation with a high-resolution model and model-data comparison, *J. Geophys. Res.*, *113*, C05024, doi:10.1029/2007JC004111.

Östlund, H. G. and G. Hut (1984), Arctic Ocean water mass balance from isotope data, *J. Geophys. Res.*, *89*, 6373–6381.

Pfirman, S., W. Haxby, H. Eicken, and M. Jeffries (2004), Drifting Arctic sea ice archives changes in ocean surface conditions, *Geophys. Res. Lett.*, *31*, L19401, doi:10.1029/2004GL020666.

Proshutinsky, A. Y. and M. A. Johnson (1997), Two circulation regimes of the wind-driven Arctic Ocean, *J. Geophys. Res.*, *102*(C6), 12,493–12,514.

Rember, R.D. and J.H. Trefry (2004), Increased concentrations of dissolved trace metals and organic carbon during snowmelt in rivers of the Alaskan Arctic, *Geochim. Cosmochim. Acta*, 68, 477-489.

Schlösser, P., R. Newton, B. Ekwurzel, S. Khatiwala, R. Mortlock, and R. Fairbanks (2002), Decrease of river runoff in the upper waters of the Eurasian Basin, Arctic Ocean, between 1991 and 1996: Evidence from $\delta^{18}\text{O}$ data, *Geophys. Res. Lett.*, 29(9), 1289, doi:10.1029/2001GL013135.

Semiletov, I., O. Dudarev, V. Luchin, A. Charkin, K.H. Shin, and N. Tanaka (2005), The East Siberian Sea as a transition zone between Pacific-derived waters and Arctic shelf waters, *Geophys. Res. Lett.*, 32, L10614, doi:10.1029/2005GL022490.

Shimada, K., E. Carmack, K. Hatakeyama, and T. Takizawa (2001), Varieties of shallow temperature maximum waters in the Western Canadian Basin of the Arctic Ocean, *Geophys. Res. Lett.*, 28, 3441–3444.

Shimada, K., M. Itoh, S. Nishino, F. McLaughlin, E. Carmack, and A. Proshutinsky (2005), Halocline structure in the Canada Basin of the Arctic Ocean, *Geophys. Res. Lett.*, 32, L03605, doi:10.1029/2004GL021358.

Shimada, K., T. Kamoshida, M. Itoh, S. Nishino, E. Carmack, F. McLaughlin, S. Zimmermann, and A. Proshutinsky (2006), Pacific Ocean inflow: Influence on catastrophic reduction of sea ice cover in the Arctic Ocean, *Geophys. Res. Lett.*, 33, L08605, doi:10.1029/2005GL025624.

Steele, M., J. Morison, W. Ermold, I. Rigor, M. Ortmeyer, and K. Shimada (2004). Circulation of summer Pacific halocline water in the Arctic Ocean, *J. Geophys. Res.*, 109, C02027, doi:10.1029/2003JC002009.

Steele, M., and W. Ermold (2004), Salinity trends on the Siberian shelves, *Geophys. Res. Lett.*, 31, L24308, doi:10.1029/2004GL021302.

Steele, M., A. Porcelli, and J. Zhang (2006), Origins of the SHEBA freshwater anomaly in the Mackenzie River Delta, *Geophys. Res. Lett.*, 33, L09601, doi:10.1029/2005GL024813.

Steele, M., and T. Boyd (1998), Retreat of the cold halocline layer in the Arctic Ocean, *J. Geophys. Res.*, 103(C5), 10,419–10,435.

Taylor, J.R., K.K. Falkner, U. Schauer, and M. Meredith (2003), Quantitative considerations of dissolved barium as a tracer in the Arctic Ocean, *J. Geophys. Res.*, 108(C12), 3374, doi:10.1029/2002JC001635.

Thompson, D.W.J. and J.M. Wallace (1998), The Arctic Oscillation signature in the wintertime geopotential height and temperature fields, *Geophys. Res. Lett.*, 25, 1297-1300.

Weingartner, T.J., S. Danielson, Y. Sasaki, V. Pavlov, and M. Kulakov (1999), The Siberian Coastal Current: a wind and buoyancy-forced arctic coastal current. *J. Geophysical Research*, *104*, 29,697 – 29,713.

Weingartner, T.J., D.J. Cavalieri, K. Aagaard, and Y. Sasaki (1998), Circulation, dense water formation and outflow on the northeast Chukchi Sea shelf, *J. Geophysical Research*, *103*, 7647-7662.

Woodgate, R.A., and K. Aagaard (2005), Revising the Bering Strait freshwater flux into the Arctic Ocean, *Geophys. Res. Lett.*, *32*, L02602, doi:10.1029/2004GL021747.

Woodgate, R.A., K. Aagaard, and T.J. Weingartner (2005), Monthly temperature, salinity and transport variability of the Bering Strait throughflow, *Geophys. Res. Lett.*, *32*, L04601, doi:10.1029/2004GL021880.

Yamamoto-Kawai, M., N. Tanaka, and S. Pivovarov (2005), Freshwater and brine behaviors in the Arctic Ocean deduced from historical data of $\delta^{18}\text{O}$ and alkalinity (1929–2002 A. D.), *J. Geophys. Res.*, *110*, C10003, doi:10.1029/2004JC002793..

Yamamoto-Kawai, M., F.A. McLaughlin, E.C. Carmack, S. Nishino, and K. Shimada (2008), Freshwater budget of the Canada Basin, Arctic Ocean, from salinity, $\delta^{18}\text{O}$, and nutrients, *J. Geophys. Res.*, *113*, C01007, doi:10.1029/2006JC003858.

Figure Captions

Figure 1. Map of sampling area and locations of hydrographic stations occupied in the Canada Basin and adjacent areas in 2003 and 2004. Capital letters indicate transects referred to in the text and subsequent figures.

Figure 2. Distributions of salinity, temperature, and dissolved Ba in the upper 200 m of the water column at stations occupied in 2003. White areas indicate locations at which dissolved Ba samples were not collected.

Figure 3. Distributions of salinity, temperature, and dissolved Ba in the upper 200 m of the water column at stations occupied in 2004.

Figure 4. Profiles of salinity, temperature and dissolved Ba at station AG occupied in the Amundsen Gulf in 2004.

Figure 5. Fractions of sea ice melt, meteoric, and saline end-members determined by salinity-oxygen isotope mass balance for samples collected in 2003. White areas indicate locations at which oxygen isotope samples were not collected.

Figure 6. Fractions of sea ice melt, meteoric, and saline end-members determined by salinity-oxygen isotope mass balance for samples collected in 2004.

Figure 7. Fractions of sea ice melt, meteoric, and saline end-members determined by salinity-oxygen isotope mass balance for samples collected at station AG occupied in the Amundsen Gulf in 2004.

Figure 8. Fractions of runoff from Eurasian and North American rivers determined from dissolved Ba and salinity-oxygen isotope mass balance for samples collected in 2003. White areas indicate locations at which samples for oxygen isotopes and/or dissolved Ba were not collected.

Figure 9. Fractions of runoff from Eurasian and North American rivers determined from dissolved Ba and salinity-oxygen isotope mass balance for samples collected in 2004.

Figure 10. Fractions of runoff from Eurasian and North American rivers determined from dissolved Ba and salinity-oxygen isotope mass balance at station AG occupied in the Amundsen Gulf in 2004.

Table 1: Salinity and oxygen isotope ratio of source waters to the upper Canada Basin.

Source	Salinity (PSS)	$\delta^{18}\text{O}$ (‰)
Sea ice melt	4 ± 1^a	-2 ± 1.0^b
Meteoric water	0	-20 ± 2^c
Pacific water	32.5 ± 0.2^d	-0.8 ± 0.1^e
Atlantic water	34.87 ± 0.03^f	0.24 ± 0.05^f

^a*Ekurzel et al., 2001.*

^b*Eicken et al., 2002; Pfirman et al., 2004.*

^c*Cooper et al., 2005.*

^d*Woodgate et al., 2005.*

^e*Yamamoto-Kawai, et al., 2008.*

^f*Yamamoto-Kawai, et al., 2005.*

Table 2: Dissolved barium concentrations in runoff from arctic rivers.

River	Discharge (km ³ yr ⁻¹)	River water dissolved Ba (nmol Ba l ⁻¹)	Effective river end-member dissolved Ba (nmol Ba l ⁻¹) ^e
<i>Eurasia</i>			
Lena	566 ^a	74 ^e 104 ^f	130
Ob	373 ^a	35-100 ^e 141 ^f	100
Yenisey	656 ^a	20-110 ^e 76 ^f	125
Kolyma	114 ^a	63 ^f	--
<i>North America</i>			
Mackenzie	322 ^b	410-425 ^e 371 ^f	520
Yukon	214 ^c	369 ^f	--
Colville	9.4 ^d	376 ± 24 ^g	--
Kuparuk	1.4 ^d	171 ± 16 ^g	--
Sagavinirktok	1.3 ^d	234 ± 14 ^g	--

^aData from Russian Federal Service of Hydrometeorology and Environment Monitoring (reported in *Cooper et al.*, 2008).

^bData from Water Survey of Canada (reported in *Cooper et al.*, 2008).

^cData from U.S. Geological Survey (reported in *Cooper et al.*, 2008).

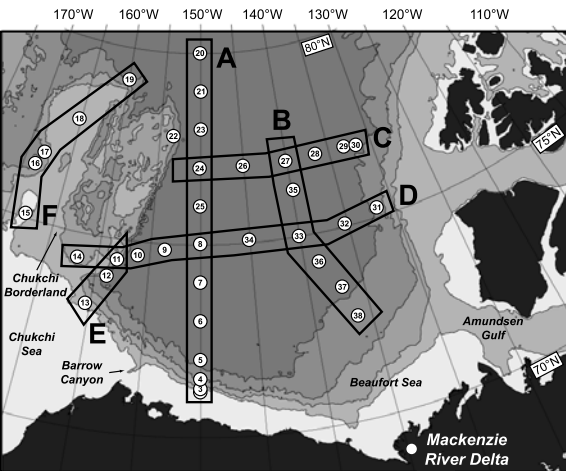
^dSurface Water data for Alaska: USGS Surface-Water Annual Statistics, National Water Information System, U.S. Geological Survey, 2008 (<http://waterdata.usgs.gov/ak/nwis/annual>)

^e*Guay and Falkner*, 1998.

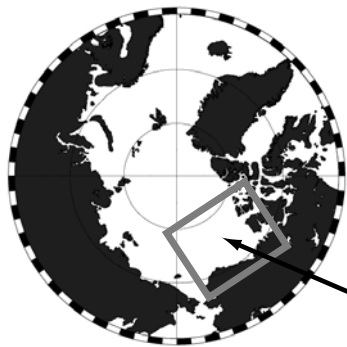
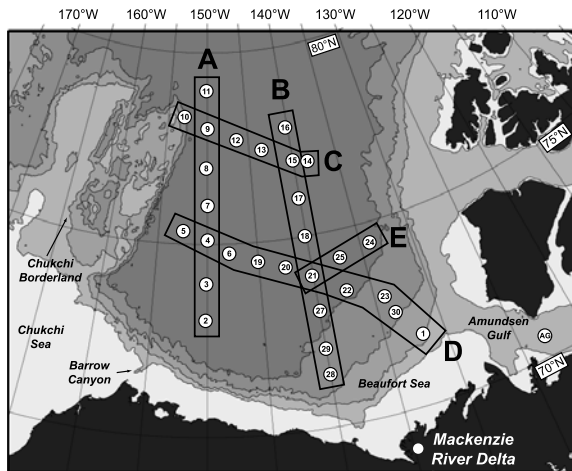
^fFlow-weighted averages [*Cooper et al.*, 2008].

^g*Rember and Trefry*, 2004.

2003 Stations (Aug 13 - Sep 3)

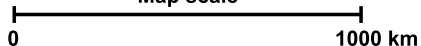


2004 Stations (Aug 5 - 29)



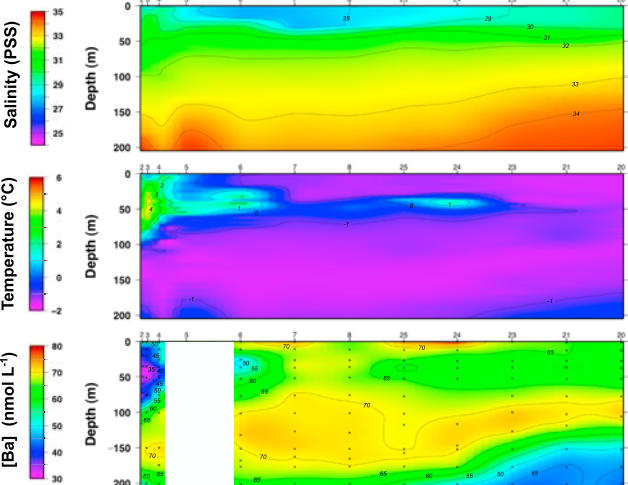
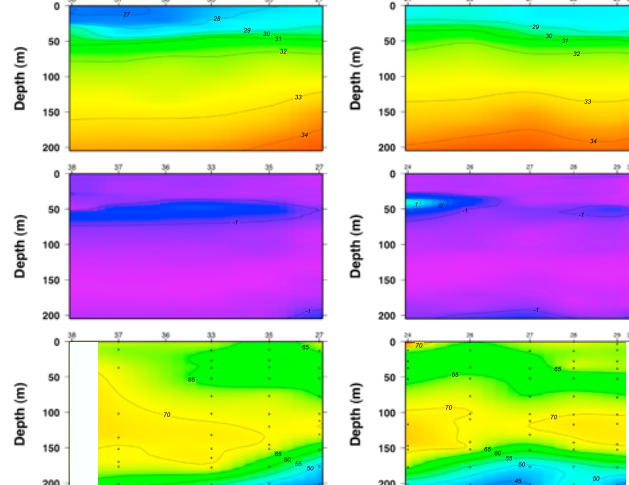
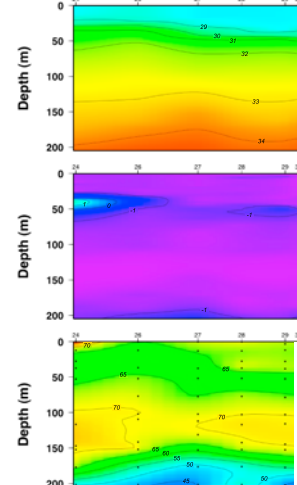
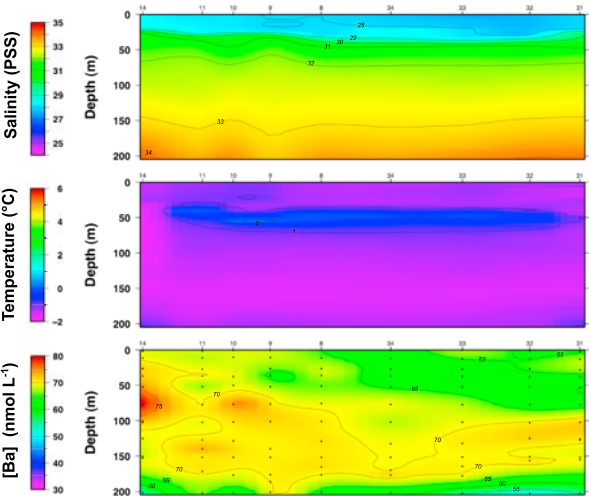
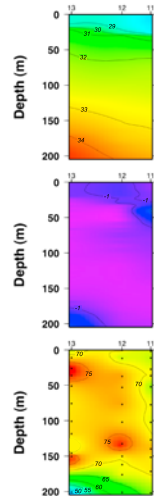
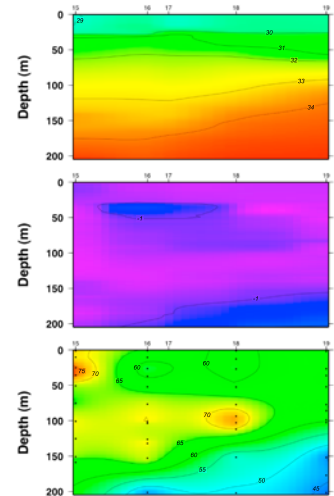
Area of map detail

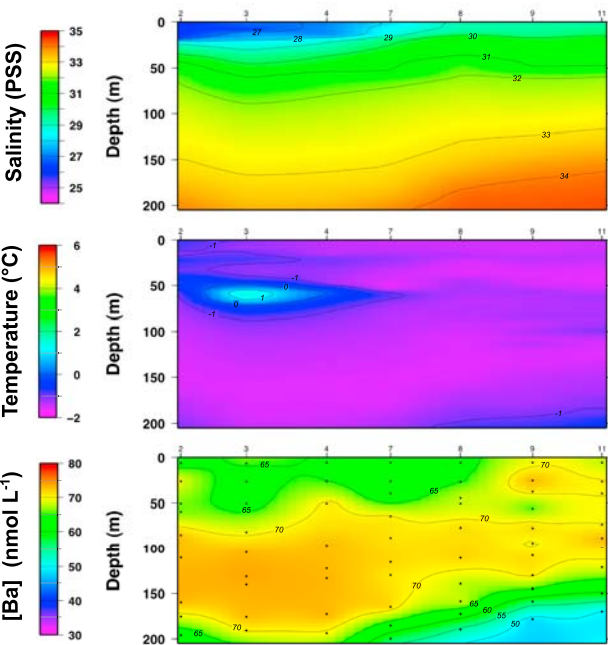
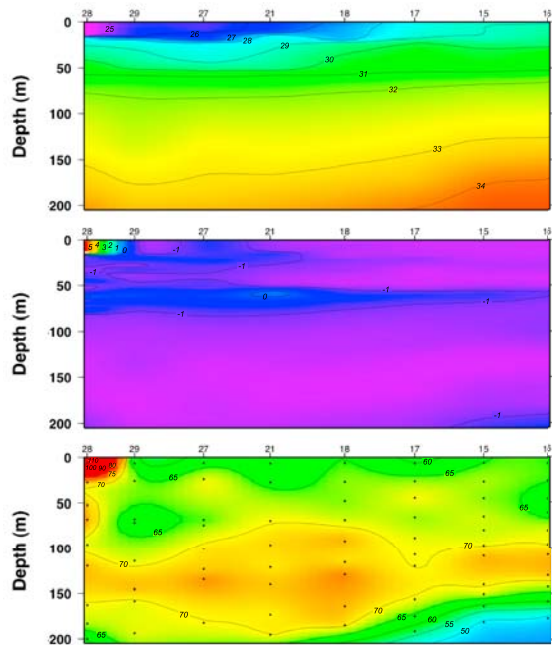
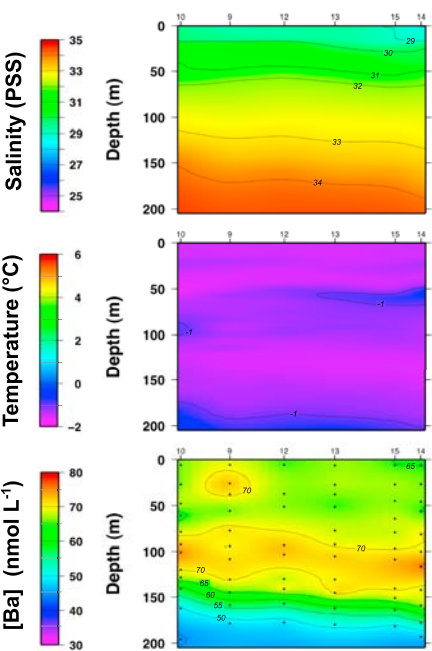
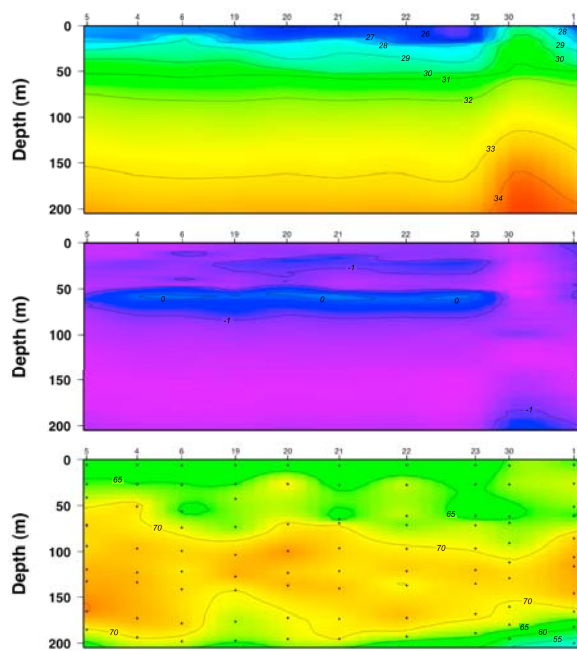
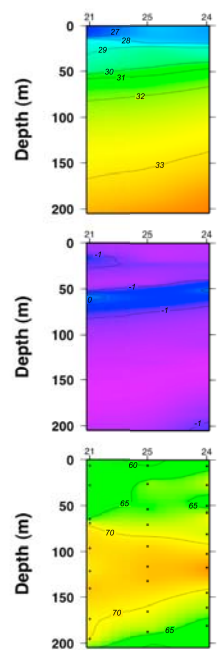
Map scale

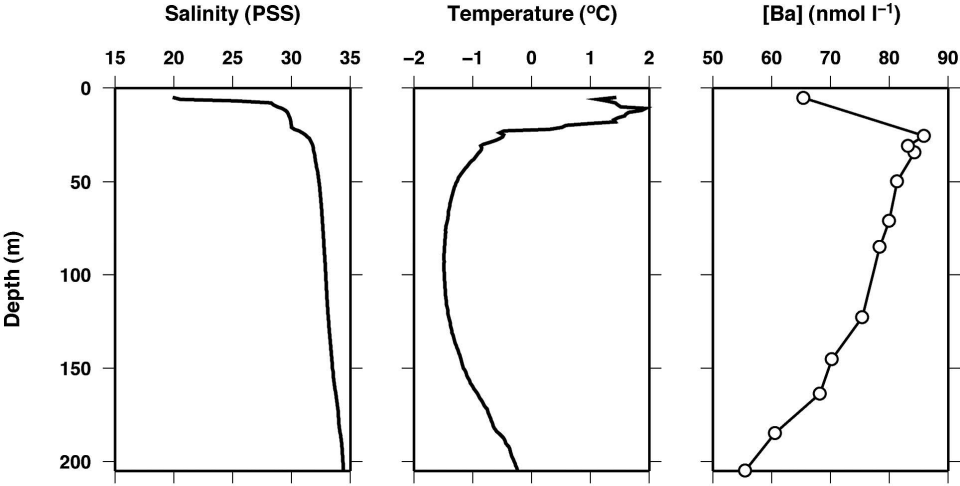


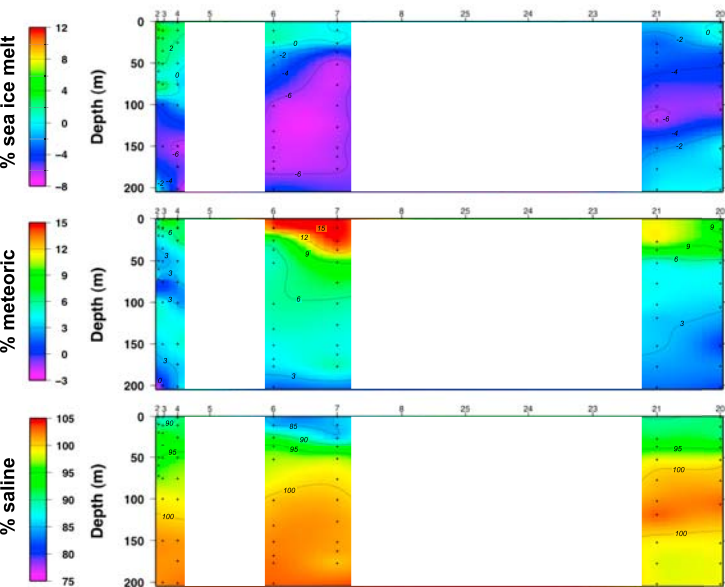
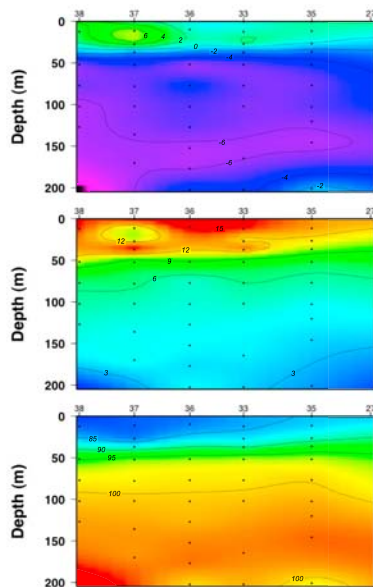
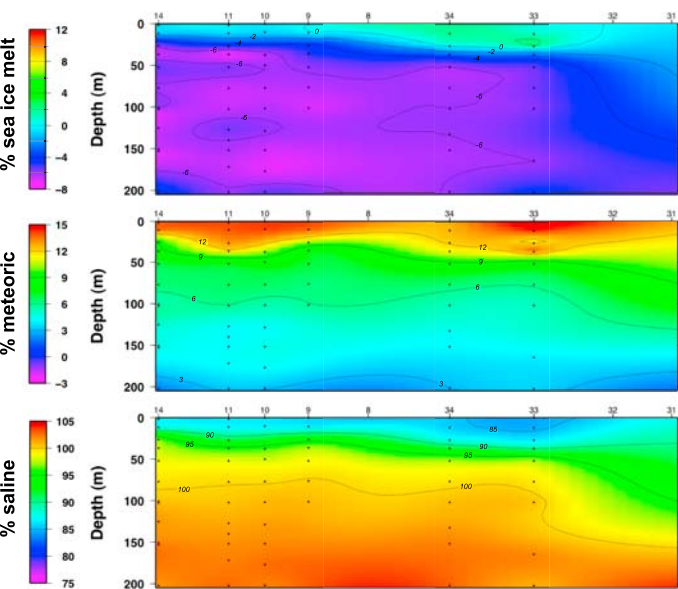
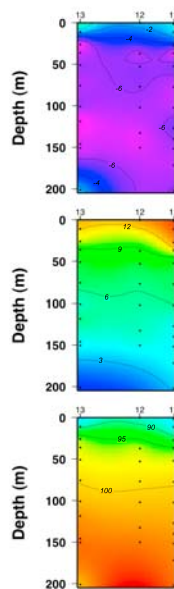
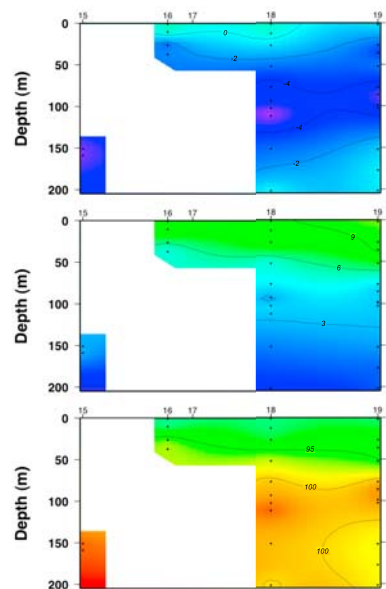
Bottom depth (meters)

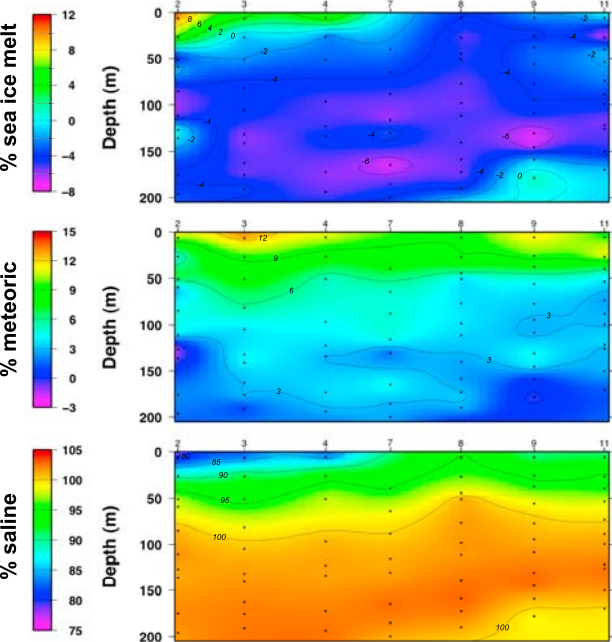
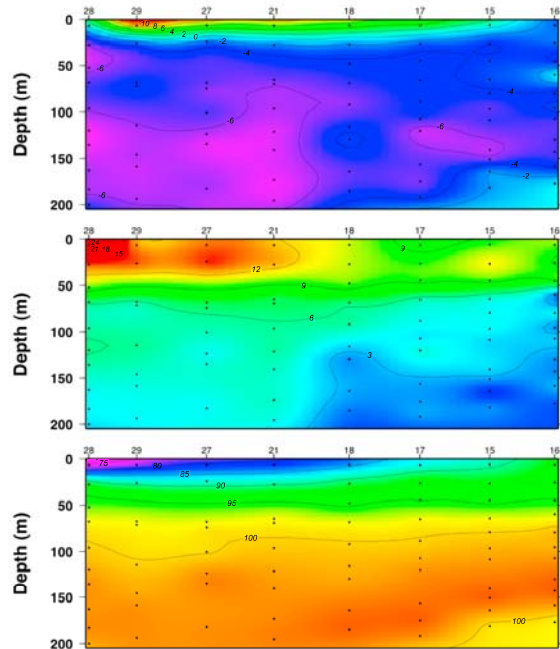
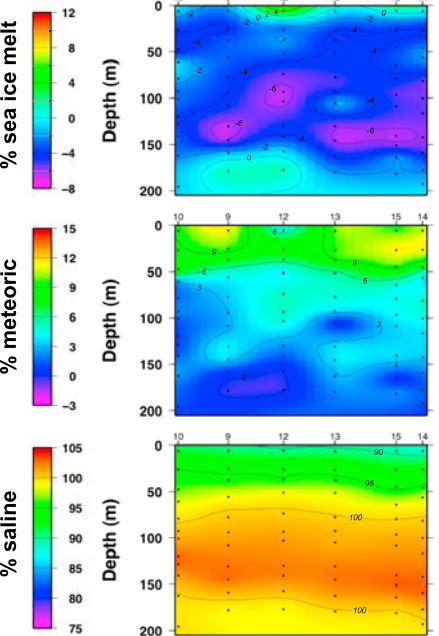
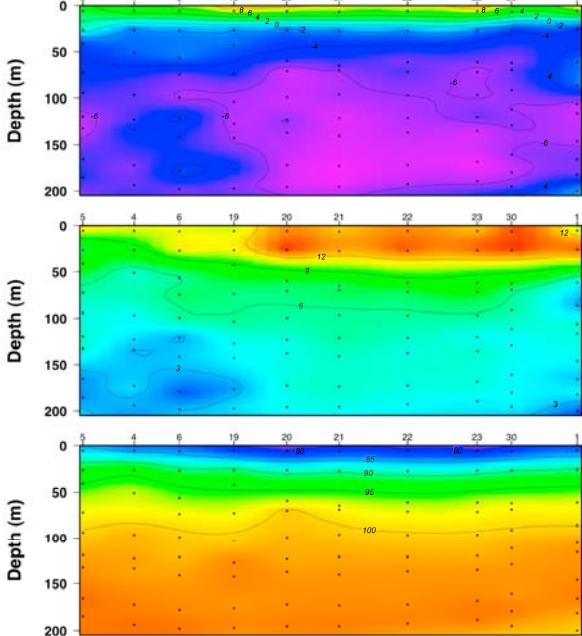
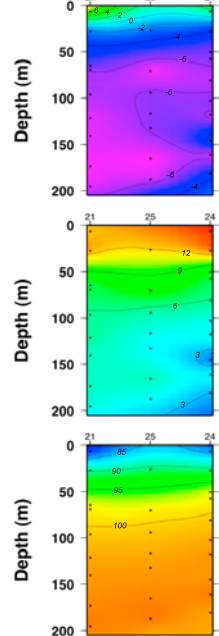


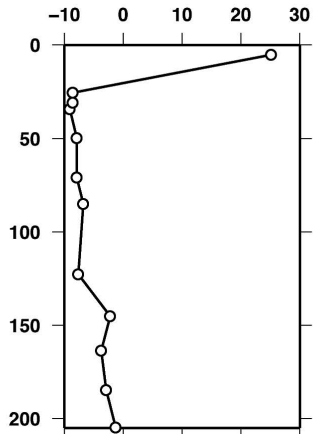
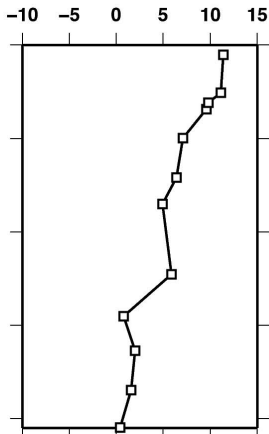
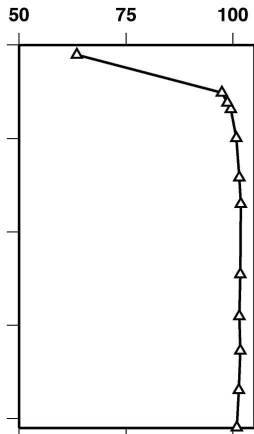
Transect A**Transect B****Transect C****Transect D****Transect E****Transect F**

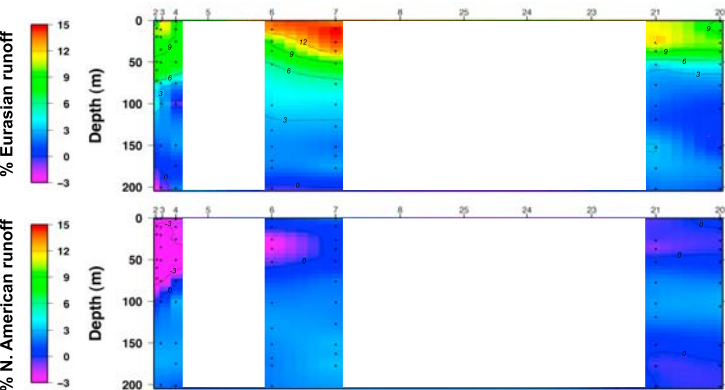
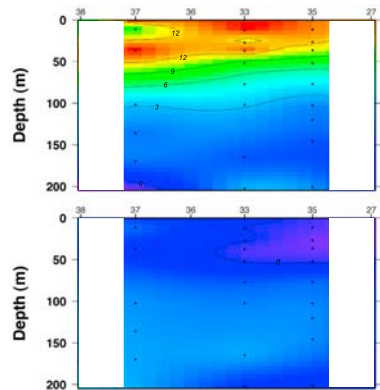
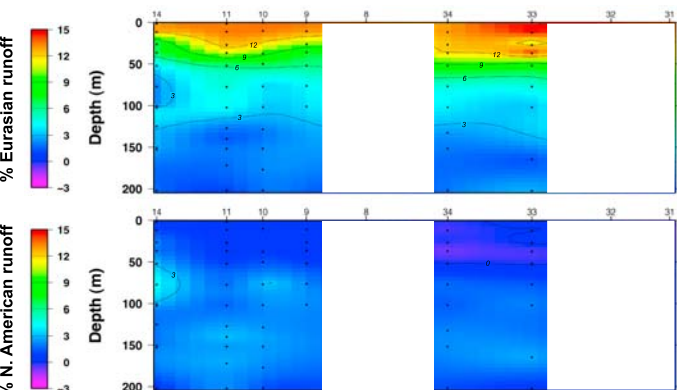
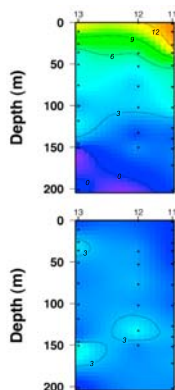
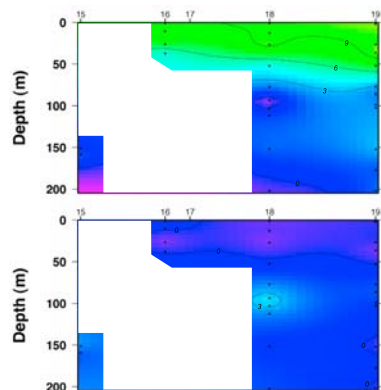
Transect A**Transect B****Transect C****Transect D****Transect E**

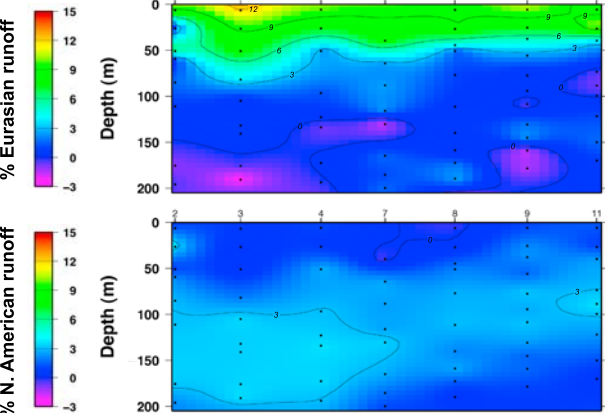
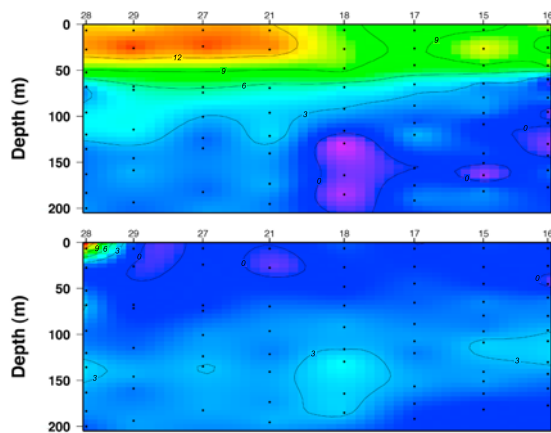
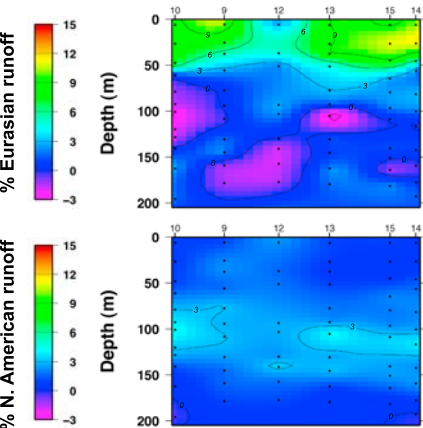
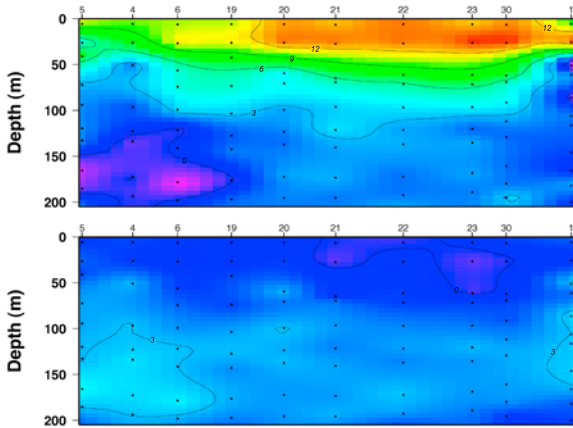
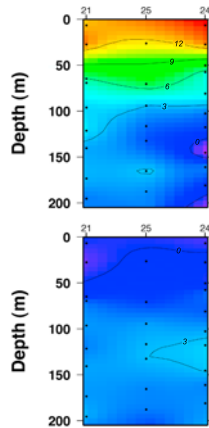


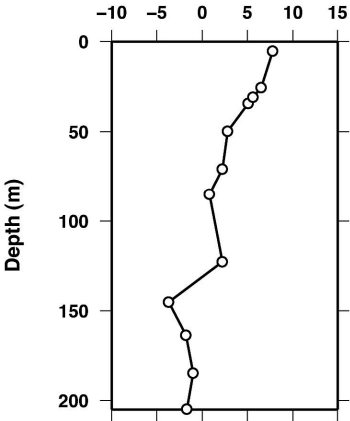
Transect A**Transect B****Transect D****Transect E****Transect F**

Transect A**Transect B****Transect C****Transect D****Transect E**

% sea ice melt**% meteoric****% saline**

Transect A**Transect B****Transect D****Transect E****Transect F**

Transect A**Transect B****Transect C****Transect D****Transect E**

% Eurasian runoff**% North American runoff**